HHS Public Access

Author manuscript

*Ann Biomed Eng*. Author manuscript; available in PMC 2019 November 01.

Published in final edited form as:

*Ann Biomed Eng*. 2018 November ; 46(11): 1911–1920. doi:10.1007/s10439-018-2077-8.

# Effects of level, loading rate, injury and repair on biomechanical response of ovine cervical intervertebral discs

**Rose G. Long**[1,2], **Ivan Zderic**[1], **Boyko Gueorguiev**[1], **Stephen Ferguson**[3], **Mauro Alini**[1], **Sibylle Grad**[1], and **James C. Iatridis**[2]

[1]AO Research Institute Davos, Clavadelstrasse 8, 7270 Davos, Switzerland [2]Department of Orthopaedics, Icahn School of Medicine at Mount Sinai, NY, NY USA [3]Institute for Biomechanics, ETH Zurich, Zürich, Switzerland

## Abstract

A need exists for pre-clinical large animal models of the spine to translate biomaterials capable of repairing intervertebral disc defects. This study characterized the effects of cervical spinal level, loading rate as well as injury and repair with genipin-crosslinked fibrin (FibGen) on axial and torsional mechanics in an ovine cervical spine model. Cervical intervertebral discs C2-C7) from 9 animals were tested with cyclic tension-compression (−240 – 100 N) and cyclic torsion (±2° & ±4°) tests at three rates (0.1, 1 & 2 Hz) in intact, injured and repaired conditions. Intact IVDs from upper cervical levels (C2-C4) had significantly higher torque range and torsional stiffness and significantly lower axial range of motion and tensile compliance than IVDs from lower cervical levels (C5-C7). A 10× increase in loading rate significantly increased torque range and torsional stiffness 4–8% (depending on amplitude) ($p < 0.001$). When normalized to intact, FibGen significantly restored torque range (FibGen: 0.96±0.14, Injury: 0.88±0.14, $p = 0.03$) and axial range of motion (FibGen: 1.00±0.05, Injury: 1.04±0.15, $p = 0.02$) compared to Injury, with a values of 1 indicating full repair. Cervical spinal level must be considered for controlling biomechanical evaluations, and FibGen restored some torsional and axial biomechanical properties to intact levels.

### Keywords

Hydrogel; biomechanics; tissue engineering; annulus fibrosus; large animal; in vitro

## Introduction

Intervertebral disc (IVD) disorders, such as defects of the annulus fibrosus (AF), are strongly associated with back and neck pain (1), a leading cause of global disability (2). Animal models of IVD disorders provide insights into disease pathology and progression

Name and Address for correspondence: James C. Iatridis, PhD, Leni & Peter W. May Department of Orthopaedics, Icahn School of Medicine at Mount Sinai, 1 Gustave Levy Place, Box 1188, New York, NY 10029-6574 USA, T 212-241-1517, F 212 876 3168, james.iatridis@mssm.edu.

**Department and Institution where work was done:** AO Research Institute Davos, Clavadelstrasse 8, 7270 Davos, Switzerland

No competing financial interests exist.

which are difficult to obtain with human clinical models due to large variability, limited availability and ethical barriers. Validation and safety testing are necessary before translating biomaterials and regenerative medicine technologies to clinical usage.

Sheep are commonly used as a model to study biochemical (3–6), structural (7,8) and biomechanical (9–11) changes to the IVD following injury. Trabecular structure and force balance analyses indicated that axial compression is the dominant loading direction in sheep, similar to the human spine (12). Intradiscal pressures in Merino sheep have been reported to be 0.5 MPa while lying and standing (13), which are very similar to those measured in human IVDs (14). Sheep IVDs have similar non-linear biomechanical responses to torsion (15) and axial loading (15,16) as human IVDs (17). The cellularity of the human IVD decreases sharply 1.5 mm into the IVD (18) due to diffusion limited nutrient and oxygen transport (19), so it is important to select an animal model with a comparable size in order to replicate its cellular, metabolic and transport environment. Ovine IVDs have a cross-sectional area of 676 $mm^2$ which is approximately 1/3 the size of human IVDs (20) and more comparable than most small animals which have IVD areas much smaller than humans. Additionally, ovine IVDs do not retain notochordal cells into adulthood (21), mirroring the human condition (22).

IVD herniation is a direct cause of back and neck pain that occurs when IVD tissue extrudes through AF defects (23). Discectomy procedures to remove this herniated tissue do not attempt to close or repair AF defects (24). Annulus repair is an unmet clinical need since 3–18% of patients require same level surgery for reherniation (25–29). Annular competence plays a role in reherniation, as patients with large annular defects (>6 mm) experience a higher reherniation risk with a rate of 27% (28). Besides contributing to reherniation risk, defects in the annulus result in altered biomechanical response (30–32), decreased cellularity (33), accelerated degeneration (34) and decreased IVD height (25). The Barricaid (Intrinsic Therapeutics, Inc., Woburn, Massachusetts), a shield within the annulus fibrosus secured to the inferior vertebral body (35) prevents reherniation (36) and protects the facet joint (37), but does not seal AF defects. Developing biomaterials that can seal AF defects is an area of active research (38). Fibrin crosslinked with genipin (FibGen) is an injectable, adhesive hydrogel that is able to seal AF defects, reduce disc height loss, and partially restore bovine IVD biomechanical function with compressive stiffness close to the intact state (39). Following these promising in vitro results, cross validation of biomechanical restoration in an alternate animal model is necessary for further translation to large animal in vivo studies.

The aim of this study was to characterize the response of intact ovine cervical IVDs to cyclic axial tension and compression in order to determine if there is an effect of cervical spinal level and loading rate. We also determined if an AF sealant could restore biomechanical properties of injured IVDs to their intact condition.

## Materials and Methods

### Study Design

Forty-five motion segments from five cervical levels (C2 through C7) of nine Swiss Alpine sheep (age range: 2–5 years, median: 3 years old) were distributed randomly in relation to

spinal level to two groups: Injured and FibGen (Figure 1). The level distribution to each group was generally balanced across level (Figure 1B). Cervical discs were used because IVD heights (6.7– 7.2 mm) are larger than thoracic (2.6–4.5 mm) and lumbar IVDs (4.2–4.5 mm) (40), and are comparable to human IVD sizes. All motion segments (hemivertebrae-disc-hemivertebrae) were first tested in the intact condition. After testing, all motion segments were injured in the dorsolateral AF region with 2 mm diameter biopsy punch that corresponded to ~30% of IVD height. The puncture depth was controlled and repeatable to a depth of 6.7mm using a plastic collar around the metal blad to control the depth. No additional nuclear material was removed. The motion segments in the Injured group were not repaired, whereas the ones in the FibGen group were repaired as follows: Genipin (Wako Chemicals USA Inc., Richmond, VA, USA) was dissolved in dimethyl sulfoxide at 6 mg/mL and 20.25 μL was added to 40 μL of 1000 U/mL thrombin (Sigma Aldrich, Buchs, Switzerland) and 226.8 μL of Phosphate Buffered Saline (PBS). The thrombin/genipin/PBS mixture was combined with 140 mg/mL fibrin (Sigma Aldrich, Buchs, Switzerland) at a volumetric ratio of 1:4 using a dual barrel syringe with mixing tip (Pearson Dental, Sylmar, CA, USA). All motion segments in both groups were then tested a second time.

## Specimen Preparation

Nine fresh-frozen ovine cervical (C1 to T1) spines were dissected of muscle and soft tissue. Using the first ribbed vertebrae as a landmark, the five cervical motion segments (C2- C7) were isolated with a transverse cut through the adjacent cranial and caudal vertebra. The posterior elements including the facet joints were removed. The motion segments were sealed and frozen individually. Individual segments were thawed at 20° C for 8 hours before testing. The proximal and distal 10 mm of each specimen were embedded in polymethylmethacrylate (PMMA, Suter Kunststoffe AG, Fraubrunnen, Switzerland).

## Biomechanical Testing and Loading Protocol

Biomechanical testing was performed on a servo-hydraulic material testing system (MiniBionix II 858, MTS Systems Corp., Eden Prairie, MN) equipped with a 25 kN/200 Nm load cell. The proximal and distal pots were firmly fixed to the machine transducer and the machine base using custom-made holders. Distally, an X-Y-table was connected between the holder and the load cell to eliminate shear forces. Each specimen was first cyclically tested under sinusoidal loading in the axial direction within a load range of 100 N tension and 240 N compression. The 240 N peak compression force generated intradiscal pressures in Merino sheep of 1.1 MPa (13). This corresponds to the pressure measured in human lumbar IVD during sitting and is higher than the pressure measured during standing and lying (14). Subsequently, the loading platen was returned to 0 N and cyclic sinusoidal torsional loading was applied to each specimen up to ± 2°, and then up to ± 4°, to mimic the limited motion of the human lumbar spine, with rotations less than 4° (41). The axial load and torsion rotations were applied at three frequencies: 0.1 Hz, 1 Hz and 2 Hz (Figure 2a). Hence, the torsional loading rates were 0.4, 4, and 8 °/s for ± 2°, and were 0.8, 8, and 16 °/s for ± 4°. Test duration was 20 cycles for all loading at 0.1 Hz, 30 cycles for 1 Hz and 100 cycles for 2 Hz (Figure 2a). At 1 and 2 Hz, the control system imposed tensile loads less than 100 N (as low as 7 N) and compressive loads greater than 250N (up to 371N), so 1 and 2 Hz data were not

analyzed. Machine data of axial load (N), axial displacement (mm), torque (Nmm) and torsional angle (°) were continuously recorded from the machine transducer at 128 Hz.

### Parameters of Interest

All parameters of interest were calculated with custom Matlab (Mathworks, Natick, MA) script using the 20$^{th}$ loading cycle. Torque range was defined as the peak to peak torque between ± 2° and ± 4° angle rotation. The torsional stiffness was calculated as the average slope of the maximum 20% of rotation of the torque-angular deformation curve in both directions (Figure 2B). No statistically significant differences in torsional stiffness were detected between clockwise and counter clockwise directions ($p>0.49$) so these parameters were averaged for a single torsional stiffness value. All axial parameters were derived from the tests performed at 0.1 Hz. The axial range of motion (ROM) was defined as the difference in axial displacement between 94 N (tension) and −227 N (compression), since this loading range was reached for all specimens. The axial compliance was calculated as the slope of the displacement-load curve at the maximum 20% of tension and compression loading (Figure 2). The compressive compliance was calculated from −196 N to −227 N and the tensile compliance from 62 N to 94 N.

### Statistics

Statistical analyses were performed using Prism version 7 for Windows (GraphPad Software, La Jolla California). The difference between FibGen and Injured was assessed with Mann-Whitney U test. The effect of level and loading rate on the biomechanical response of intact specimens was assessed with Friedman test and Dunn's test (42) for multiple comparisons. All data were presented median ± interquartile range. Significant differences were determined with $p < 0.05$ and statistical trends were reported with $0.05 \leq p < 0.10$.

## Results

### Effect of Level

The two cranial (C2-C3 and C3-C4) IVD levels (n = 9 per level) had a distinct torsional and axial biomechanical response compared to the caudal levels (C5-C6 and C6-C7). The axial ROM of C2-C3 (median: 0.99 mm, interquartile range: 0.83– 1.0 mm) was significantly lower compared to the three caudal levels C4-C5 (1.5 mm, 1.2– 1.7 mm), C5-C6 (1.4 mm, 1.3 – 1.7 mm) and C6-C7 (1.7 mm, 1.5 – 2.0 mm). In addition, C3-C4 (1.1 mm, 0.89 – 1.2 mm) revealed significantly lower axial ROM than C5-C6 and C6-C7 (Figure 3A-B). The tensile compliance of C2-C3 (4.6 μm/N, 4.3 – 5.7 μm/N) was significantly less than C5-C6 (6.3 μm/N, 5.5 – 7.1 μm/N) and C6-C7 levels (7.4 μm/N, 5.8 – 7.9 μm/N) ($p<0.05$), and the tensile compliance between C3- C4 (4.6 μm/N, 4.3 – 5.7 μm/N) and C5-C6 showed a trend to difference ($p = 0.07$) (Figure 3C). There were no significant differences in compressive compliance between levels (Figure 3D).

The ± 2° and ± 4° torque range of C2-C3 and C3-C4 were significantly larger than C5-C6 and C6-C7 ($p< 0.05$) (Figure 4A-F). The ± 2° and ± 4° torsional stiffness of C2-C3 and C3-

C4 were significantly larger than the C5-C6 and C6-C7 ($p < 0.05$) (Figure 4A-F). The ± 4° torsional stiffness of C3-C4 was significantly higher than C4-C5 ($p<0.05$).

### Effect of Loading Rate

The torque range and torsional stiffness for both rotations, ± 2° and ± 4°, increased as loading rate increased (n = 45) (Figure 5A-D). The torque range for ± 2° increased significantly from 0.4 °/s to 4 °/s and to 8 °/s ($p < 0.05$) (Figure 5A). The torsional stiffness increased significantly the loading rate increased from 0.4 °/s to 4 °/s, and for 8 °/s ($p < 0.05$) (Figure 5B).

The torque range of ± 4° increased significantly by 4% as loading rate increased from 0.8 °/s to 8 °/s and by 5% as it increased to 16 °/s ($p < 0.05$) (Figure 5C). The torsional stiffness for ± 4° increased significantly by 8% as the loading rate increased from 0.8 °/s to 8 °/s, and 12% for 16 °/s ($p < 0.05$) (Figure 5D).

### Effect of Injury and Repair

The relative effects of injury (Injured group, n = 22) and FibGen repair (FibGen group, n = 23) on intact biomechanics were assessed by normalizing the value of the second test to the value of the first test (intact condition). The axial range of motion ratio was significantly lower for the FibGen group (1.00, 0.95–1.04) than for the Injured group (1.06, 1.00 – 1.10) ($p < 0.05$) (Figure 6A). However, there was no significant difference in tensile and compressive compliance ratios between FibGen and Injured groups ($p = 0.12$ and $p = 0.11$, respectively) (Figures 6B-C).

The ± 2° torque range ratio was significantly higher for the FibGen group (0.85, 0.66–0.95) compared to the Injured group (0.81, 0.62 – 0.86) ($p<0.05$) (Figure 7). The average torsional stiffness ± 2° trended to higher values for the FibGen group (0.93, 0.88–1.01) compared to Injured (0.88, 0.82 – 0.94) ($p = 0.09$) (Figure 7A-B).

The torque range ratio for ± 4° for the FibGen group (0.95, 0.84 – 0.99) revealed a trend to difference compared to the Injured group (0.91, 0.67 – 0.94) ($p=0.09$) (Figure 7C). Under ± 4° loading, the torsional stiffness ratio did not significantly differ between the FibGen and Injured groups ($p = 0.51$).

## Discussion

This ex-vivo study characterized the biomechanical response of ovine cervical IVDs to assess the effects of spinal level, loading rate, injury and repair. Of these three variables, spinal level had the greatest effect followed by injury and loading rate. The two most cranial cervical levels (C2-C3 and C3-C4) of the Swiss Alpine sheep had higher torque range, higher torsional stiffness, lower axial range of motion and lower compressive compliance than the two most caudal levels (C5-C6 and C6-C7). The faster loading rates were associated with increased torque range and increased torsional stiffness. The 2mm biopsy punch increased mobility as seen with decreased torque range, decreased torsional stiffness, increased range of motion and increased axial compliance compared to the intact condition. The FibGen repair reduced these changes for ± 2° torque range and axial range of motion.

The biomechanical parameters found in this study are comparable to other ovine studies although direct comparison can be difficult due to differences in testing protocols, specimen preparation, parameter definitions and normalizations. A comparison of female Rambouillet-Columbia sheep lumbar IVDs and human lumbar IVDs found a compressive compliance of 0.6 μm/N (1432 N/mm) for sheep (16), which is approximately half of what our study found (1.4–1.7 μm/N). A multiple regression model between the independent variables axial preload and rotation angle, and dependent torsion mechanics parameters (i.e. torsional stiffness, hysteresis height and apparent torsional modulus) highlights that torsional stiffness is increased with axial preload, and can facilitate comparisons of torsion mechanical parameters across studies with different loading protocols (43). A separate study of torsional mechanics of the lumbar IVDs from sheep measured torsional stiffness of 3000 Nmm/°, defined as the slope of the torque rotation curve in the rotation angle range of 4.5–5.5° with 0.48 MPa preload (15). We found a lower torsional stiffness of 673 ± 324 Nmm/°, but this may be because it was calculated at lower range of 3.6°– 4° and with no preload. In the same study, the average torque range measured up to 6° was 15,000 Nmm (15), which is approximately five times higher than this study, where torque range from ±4° was 3,300 Nmm. Differences between lumbar and cervical levels may also contribute since lumbar ovine IVDs have less IVD height and larger area than the cervical IVDs (40).

IVD biomechanical behaviors are known to depend on spinal level in the literature, although the bimodal distribution seen in this study has not been reported and is likely associated with different mechanical roles of upper and lower cervical spine levels. In flexibility testing of whole Merino sheep cervical spines, the respective resultant rotation of each cervical level, starting with C2-C3, was 2.75°, 5.56°, 6.51°, 8.4° and 11.1° with axial rotation moment of ± 2500 Nmm, suggesting linearly increasing range of motion with C3-C4 and C4-C5 most similar (44).Similarly, we found decreased torque range with increased level, but we found the torque range of two most cranial (C2-C3 and C3-C4) were similar to each other and were 100% greater than the two most caudal levels (C5-C6 and C6-C7). Anatomical data of vertebral bodies of Merino sheep suggest cross sectional area does not explain this variability, since the inferior endplate width of C3-C4 (25.8 ± 1.0 mm) is 10% larger than C5-C6 (23.4 ± 1.1 mm) and18% larger than to C6-C7 (21.8 ± 1.6 mm) (40). The large spinal level effect and small geometry variation suggests geometry does do not fully account for the pattern observed in this study, and indicates there may be variation in material properties due to spine level dependent mechanical demands. Reitmaier et al. found that sheep lumbar spines had comparable intradiscal pressures across spinal level (L2-L3 and L4-L5) for lying, sleeping, standing, lying down and walking activities, although L2-L3 had approximately 20% less intradiscal pressure when standing up from sitting than the L4-L5 (13). One study using MRI to estimate GAG content found lower GAG in more cranial cervical discs (45), so there may be a biochemical basis for our findings. The significant and large differences in mechanical behaviors between cervical spinal levels highlights the importance of using level matched controls for preclinical evaluation of injury and treatment effects, particularly when including upper cervical IVD levels.

Annular injury significantly decreased torque range and increased axial ROM in this study, suggesting destabilization, and builds upon similar changes observed in different injury models (46). We used a 2mm diameter defect measuring approximately 30% of IVD height.

This relative defect size roughly represents the majority of patients; fifty percent of patients have defect with diameter less than 50% of disc height while the remaining patients had larger defects (17%) or no observable defect (32%) (28,47). In this study, the effect size from a 2-mm biopsy punch injury on torsional and axial parameters ranged from 1–15%, depending on the parameter measured. The biomechanical changes from annulus injury support previously reported reduced torsional stiffness and IVD height after vertical and rim annular incision (30). In a separate study, the reduction in compressive stiffness and torsion stiffness compared to pre- injury scaled with needle size (31). A needle puncture in the annulus causes a reduction of compressive stiffness, tensile stiffness, neutral zone stiffness and neutral zone length that was dependent on needle gauge size (48). FibGen repair reduced the change in torque range and axial ROM induced by puncture injury in this study. Previous biomechanical studies showed that FibGen reduced disc height loss from injury in a bovine organ culture model, restored compressive stiffness, (49) and restored multiple rotational flexibility measurements (50). The restoration of multiple aspects of biomechanical response to intact levels supports future in vivo evaluation of FibGen using live animal testing with the ovine model presented here.

There are some limitations of this study. Injured and FibGen groups are distributed relatively evenly across level (Figure 1 B), although the effect of injury and FibGen repair did fully control for the effect of level, so if C2-C3 responds very differently to injury than C5-C6, the results may be confounded. A biopsy punch was used to create a uniform size, shape and depth of injury across all specimens, although this injury was done by hand and could be a source of some variation. We used an axial compressive load of 250N which corresponds to 1.1 MPa axial stress measured in the ovine lumbar spine. This load magnitude corresponds to physiological loading in the human lumbar spine where the biomaterials are anticipated for application, but in vivo loads in the ovine cervical spine are not well known. Torsional mechanics were measured without an axial preload, which is always present *in vivo*, and is known to increase motion segment stiffness (51). As a result, torsional stiffness values presented here may be lower than expected under pre-load conditions. There was one sample that exhibited an irregular axial response during the intact axial testing. While slipping between the machine clamps and plastic embedding could explain this finding, the data traces did not exhibit obvious slipping effects. The data was included because it was not considered a statistical outlier, and because its removal would require removal of a whole animal. All axial parameters were derived from 0.1 Hz tests because the test system did not adequately control to the target waveform with at higher rates of loading with lower tension loads (as low as 7N) and higher compressive loads (up to - 371N) at 1 and 2 Hz. The recovery time for samples in both groups was comparable, but we did not measure the effect of recovery with a control no injury group, so there may be unmeasured recovery effects. This study focused on the capacity of FibGen to restore biomechanical behaviors of ovine cervical motion segments, and future studies are required to determine risk of implant expulsion with in vivo studies and/or in vitro studies, for example using the rigorous cyclic complex loading conditions previously described(52).

In conclusion, this biomechanical study showed that spinal level, disc injury and loading frequency had significant effects on ovine cervical IVD biomechanical behavior. Spinal level had the largest effect, highlighting the importance of accounting for level effects in study

design. The increase in loading rate by a factor of 10 and 20 resulted in only a small increase in torque range and torsional stiffness, indicating that viscous effects in the ovine IVD are modest in this range of loading rates. The 2-mm biopsy punch reduced ±2° torque range by 15% and increased axial range of motion by 5%, and these changes were reversed with FibGen repair, highlighting the promise of this injectable adhesive for AF repair. Together, these results characterize the Swiss Alpine sheep as a model of annulus injury and repair and help inform future therapeutic and study design decisions.

## Acknowledgments

This research was funded by National Institute for Arthritis and Musculoskeletal and Skin Diseases (R01AR057397), the Whitaker Foundation, and a Collaborative Research Partner Program grant on Annulus Fibrosus Rupture from the AO Foundation, Davos, Switzerland. The authors gratefully acknowledge important technical contributions of Patrick Hörnlimann and Dieter Wahl.

## References

1. Livshits G, Popham M, Malkin I, Sambrook PN, Macgregor AJ, Spector T, et al. Lumbar disc degeneration and genetic factors are the main risk factors for low back pain in women: the UK Twin Spine Study. Ann Rheum Dis. 2011 Oct; 70(10):1740–1745. [PubMed: 21646416]
2. GBD 2015 DALYs and HALE Collaborators. Global, regional, and national disability-adjusted life-years (DALYs) for 315 diseases and injuries and healthy life expectancy (HALE), 1990–2015: a systematic analysis for the Global Burden of Disease Study 2015. The Lancet. 2016 Oct 8; 388(10053):1603–1658.
3. Melrose J, Ghosh P, Taylor TK. A comparative analysis of the differential spatial and temporal distributions of the large (aggrecan, versican) and small (decorin, biglycan, fibromodulin) proteoglycans of the intervertebral disc. J Anat. 2001 Jan; 198(Pt 1):3–15. [PubMed: 11215765]
4. Melrose J, Ghosh P, Taylor TK, Hall A, Osti OL, Vernon-Roberts B, et al. A longitudinal study of the matrix changes induced in the intervertebral disc by surgical damage to the annulus fibrosus. J Orthop Res. 1992 Sep; 10(5):665–676. [PubMed: 1500980]
5. Shu C, Hughes C, Smith SM, Smith MM, Hayes A, Caterson B, et al. The ovine newborn and human foetal intervertebral disc contain perlecan and aggrecan variably substituted with native 7D4 CS sulphation motif: spatiotemporal immunolocalisation and co-distribution with Notch-1 in the human foetal disc. Glycoconj J. 2013 Oct; 30(7):717–725. [PubMed: 23756834]
6. Melrose J, Ghosh P, Taylor TK, Vernon-Roberts B, Latham J, Moore R. Elevated synthesis of biglycan and decorin in an ovine annular lesion model of experimental disc degeneration. Eur Spine J. 1997; 6(6):376–384. [PubMed: 9455664]
7. Melrose J, Smith SM, Little CB, Moore RJ, Vernon-Roberts B, Fraser RD. Recent advances in annular pathobiology provide insights into rim-lesion mediated intervertebral disc degeneration and potential new approaches to annular repair strategies. Eur Spine J. 2008 Sep; 17(9):1131–1148. [PubMed: 18584218]
8. Melrose J, Roberts S, Smith S, Menage J, Ghosh P. Increased nerve and blood vessel ingrowth associated with proteoglycan depletion in an ovine anular lesion model of experimental disc degeneration. Spine. 2002 Jun 15; 27(12):1278–1285. [PubMed: 12065974]
9. Melrose J, Shu C, Young C, Ho R, Smith MM, Young AA, et al. Mechanical destabilization induced by controlled annular incision of the intervertebral disc dysregulates metalloproteinase expression and induces disc degeneration. Spine. 2012 Jan 1; 37(1):18–25. [PubMed: 22179320]
10. Reitmaier S, Volkheimer D, Berger-Roscher N, Wilke H-J, Ignatius A. Increase or decrease in stability after nucleotomy? Conflicting in vitro and in vivo results in the sheep model. J R Soc Interface. 2014 Nov 6.11(100):20140650. [PubMed: 25209401]
11. Reitmaier S, Schuelke J, Schmidt H, Volkheimer D, Ignatius A, Wilke H-J. Spinal fusion without instrumentation - Experimental animal study. Clin Biomech (Bristol, Avon). 2017 Jul.46:6–14.

12. Smit TH. The use of a quadruped as an in vivo model for the study of the spine - biomechanical considerations. Eur Spine J. 2002 Apr; 11(2):137–144. [PubMed: 11956920]
13. Reitmaier S, Schmidt H, Ihler R, Kocak T, Graf N, Ignatius A, et al. Preliminary investigations on intradiscal pressures during daily activities: an in vivo study using the merino sheep. PLoS ONE. 2013 Jul 24.8(7):e69610. [PubMed: 23894509]
14. Long RG, Torre OM, Hom WW, Assael DJ, Iatridis JC. Design requirements for annulus fibrosus repair: review of forces, displacements, and material properties of the intervertebral disk and a summary of candidate hydrogels for repair. J Biomech Eng. 2016 Feb.138(2):021007. [PubMed: 26720265]
15. Showalter BL, Beckstein JC, Martin JT, Beattie EE, Espinoza Orías AA, Schaer TP, et al. Comparison of animal discs used in disc research to human lumbar disc: torsion mechanics and collagen content. Spine. 2012 Jul 1; 37(15):E900–7. [PubMed: 22333953]
16. Beckstein JC, Sen S, Schaer TP, Vresilovic EJ, Elliott DM. Comparison of Animal Discs Used in Disc Research to Human Lumbar Disc. Spine. 2008 Mar; 33(6):E166–E173. [PubMed: 18344845]
17. Costi JJ, Stokes IA, Gardner-Morse MG, Iatridis JC. Frequency-dependent behavior of the intervertebral disc in response to each of six degree of freedom dynamic loading: solid phase and fluid phase contributions. Spine. 2008 Jul 15; 33(16):1731–1738. [PubMed: 18628705]
18. Maroudas A, Stockwell RA, Nachemson A, Urban J. Factors involved in the nutrition of the human lumbar intervertebral disc: cellularity and diffusion of glucose in vitro. J Anat. 1975 Sep; 120(Pt 1):113–130. [PubMed: 1184452]
19. Horner HA, Urban JP. 2001 Volvo Award Winner in Basic Science Studies: Effect of nutrient supply on the viability of cells from the nucleus pulposus of the intervertebral disc. Spine. 2001 Dec 1; 26(23):2543–2549. [PubMed: 11725234]
20. O'Connell GD, Vresilovic EJ, Elliott DM. Comparison of animals used in disc research to human lumbar disc geometry. Spine. 2007 Feb 1; 32(3):328–333. [PubMed: 17268264]
21. Melrose J, Smith S, Ghosh P. Assessment of the cellular heterogeneity of the ovine intervertebral disc: comparison with synovial fibroblasts and articular chondrocytes. Eur Spine J. 2003 Feb; 12(1):57–65. [PubMed: 12592548]
22. Trout JJ, Buckwalter JA, Moore KC, Landas SK. Ultrastructure of the human intervertebral disc. I. Changes in notochordal cells with age. Tissue Cell. 1982; 14(2):359–369. [PubMed: 7202266]
23. Moore RJ, Vernon-Roberts B, Fraser RD, Osti OL, Schembri M. The origin and fate of herniated lumbar intervertebral disc tissue. Spine. 1996 Sep 15; 21(18):2149–2155. [PubMed: 8893441]
24. Guterl CC, See EY, Blanquer SBG, Pandit A, Ferguson SJ, Benneker LM, et al. Challenges and strategies in the repair of ruptured annulus fibrosus. Eur Cell Mater. 2013 Jan 2.25:1–21. [PubMed: 23283636]
25. McGirt MJ, Eustacchio S, Varga P, Vilendecic M, Trummer M, Gorensek M, et al. A prospective cohort study of close interval computed tomography and magnetic resonance imaging after primary lumbar discectomy: factors associated with recurrent disc herniation and disc height loss. Spine. 2009 Sep 1; 34(19):2044–2051. [PubMed: 19730212]
26. Carragee EJ, Spinnickie AO, Alamin TF, Paragioudakis S. A prospective controlled study of limited versus subtotal posterior discectomy: short-term outcomes in patients with herniated lumbar intervertebral discs and large posterior anular defect. Spine. 2006 Mar 15; 31(6):653–657. [PubMed: 16540869]
27. Barth M, Diepers M, Weiss C, Thomé C. Two-year Outcome After Lumbar Microdiscectomy: Part 2: Radiographic Evaluation and Correlation With Clinical Outcome. Spine. 2008
28. Carragee EJ, Han MY, Suen PW, Kim D. Clinical outcomes after lumbar discectomy for sciatica: the effects of fragment type and anular competence. J Bone Joint Surg Am. 2003 Jan; 85-A(1): 102–108. [PubMed: 12533579]
29. Daneyemez M, Sali A, Kahraman S, Beduk A, Seber N. Outcome analyses in 1072 surgically treated lumbar disc herniations. Minim Invasive Neurosurg. 1999 Jun; 42(2):63–68. [PubMed: 10422699]
30. Michalek AJ, Iatridis JC. Height and torsional stiffness are most sensitive to annular injury in large animal intervertebral discs. Spine J. 2012 May 22; 12(5):425–432. [PubMed: 22627276]

31. Michalek AJ, Funabashi KL, Iatridis JC. Needle puncture injury of the rat intervertebral disc affects torsional and compressive biomechanics differently. Eur Spine J. 2010 Dec; 19(12):2110–2116. [PubMed: 20544231]
32. Haughton VM, Rogers B, Meyerand ME, Resnick DK. Measuring the axial rotation of lumbar vertebrae in vivo with MR imaging. AJNR Am J Neuroradiol. 2002 Aug; 23(7):1110–1116. [PubMed: 12169466]
33. Iatridis JC, Michalek AJ, Purmessur D, Korecki CL. Localized intervertebral disc injury leads to organ level changes in structure, cellularity, and biosynthesis. Cell Mol Bioeng. 2009 Sep 1; 2(3): 437–447. [PubMed: 21179399]
34. Masuda K, Aota Y, Muehleman C, Imai Y, Okuma M, Thonar EJ, et al. A novel rabbit model of mild, reproducible disc degeneration by an anulus needle puncture: correlation between the degree of disc injury and radiological and histological appearances of disc degeneration. Spine. 2005 Jan 1; 30(1):5–14. [PubMed: 15626974]
35. Bouma GJ, Barth M, Ledic D, Vilendecic M. The high-risk discectomy patient: prevention of reherniation in patients with large anular defects using an anular closure device. Eur Spine J. 2013 May; 22(5):1030–1036. [PubMed: 23377540]
36. Parker SL, Grahovac G, Vukas D, Vilendecic M, Ledic D, McGirt MJ, et al. Effect of an Annular Closure Device (Barricaid) on Same-Level Recurrent Disk Herniation and Disk Height Loss After Primary Lumbar Discectomy: Two-year Results of a Multicenter Prospective Cohort Study. Clin Spine Surg. 2016 Dec; 29(10):454–460. [PubMed: 27879508]
37. Trummer M, Eustacchio S, Barth M, Klassen PD, Stein S. Protecting facet joints post-lumbar discectomy: Barricaid annular closure device reduces risk of facet degeneration. Clin Neurol Neurosurg. 2013 Aug; 115(8):1440–1445. [PubMed: 23473658]
38. Bowles RD, Setton LA. Biomaterials for intervertebral disc regeneration and repair. Biomaterials. 2017 Mar 15.129:54–67. [PubMed: 28324865]
39. Schek RM, Michalek AJ, Iatridis JC. Genipin-crosslinked fibrin hydrogels as a potential adhesive to augment intervertebral disc annulus repair. Eur Cell Mater. 2011 Apr 18.21:373–383. [PubMed: 21503869]
40. Wilke HJ, Kettler A, Wenger KH, Claes LE. Anatomy of the sheep spine and its comparison to the human spine. Anat Rec. 1997 Apr; 247(4):542–555. [PubMed: 9096794]
41. Pearcy MJ, Tibrewal SB. Axial rotation and lateral bending in the normal lumbar spine measured by three-dimensional radiography. Spine. 1984; 9(6):582–587. [PubMed: 6495028]
42. Dunn OJ. Multiple comparisons using rank sums. Technometrics. 1964 Aug; 6(3):241–252.
43. Bezci SE, Klineberg EO, O'Connell GD. Effects of axial compression and rotation angle on torsional mechanical properties of bovine caudal discs. J Mech Behav Biomed Mater. 2018 Jan. 77:353–359. [PubMed: 28965042]
44. Wilke HJ, Kettler A, Claes LE. Are sheep spines a valid biomechanical model for human spines? Spine. 1997 Oct 15; 22(20):2365–2374. [PubMed: 9355217]
45. Schleich C, Müller-Lutz A, Zimmermann L, Boos J, Schmitt B, Wittsack H-J, et al. Biochemical imaging of cervical intervertebral discs with glycosaminoglycan chemical exchange saturation transfer magnetic resonance imaging: feasibility and initial results. Skeletal Radiol. 2016 Jan; 45(1):79–85. [PubMed: 26377579]
46. Iatridis JC, Nicoll SB, Michalek AJ, Walter BA, Gupta MS. Role of biomechanics in intervertebral disc degeneration and regenerative therapies: what needs repairing in the disc and what are promising biomaterials for its repair? Spine J. 2013 Mar; 13(3):243–262. [PubMed: 23369494]
47. Busscher I, Ploegmakers JJW, Verkerke GJ, Veldhuizen AG. Comparative anatomical dimensions of the complete human and porcine spine. Eur Spine J. 2010 Jul; 19(7):1104–1114. [PubMed: 20186441]
48. Elliott DM, Yerramalli CS, Beckstein JC, Boxberger JI, Johannessen W, Vresilovic EJ. The effect of relative needle diameter in puncture and sham injection animal models of degeneration. Spine. 2008 Mar 15; 33(6):588–596. [PubMed: 18344851]
49. Likhitpanichkul M, Dreischarf M, Illien-Junger S, Walter BA, Nukaga T, Long RG, et al. Fibrin-genipin adhesive hydrogel for annulus fibrosus repair: performance evaluation with large animal

organ culture, in situ biomechanics, and in vivo degradation tests. Eur Cell Mater. 2014 Jul 18.28:25–37. discussion 37. [PubMed: 25036053]

50. Long RG, Bürki A, Zysset P, Eglin D, Grijpma DW, Blanquer SBG, et al. Mechanical Restoration and Failure Analyses of Composite Repair Strategy for Annulus Fibrosus. Acta Biomater. 2015:1–30.
51. Gardner-Morse MG, Stokes IA. Physiological axial compressive preloads increase motion segment stiffness, linearity and hysteresis in all six degrees of freedom for small displacements about the neutral posture. J Orthop Res. 2003 May; 21(3):547–552. [PubMed: 12706030]
52. Wilke H-J, Ressel L, Heuer F, Graf N, Rath S. Can prevention of a reherniation be investigated? Establishment of a herniation model and experiments with an anular closure device. Spine. 2013 May 1; 38(10):E587–93. [PubMed: 23429676]

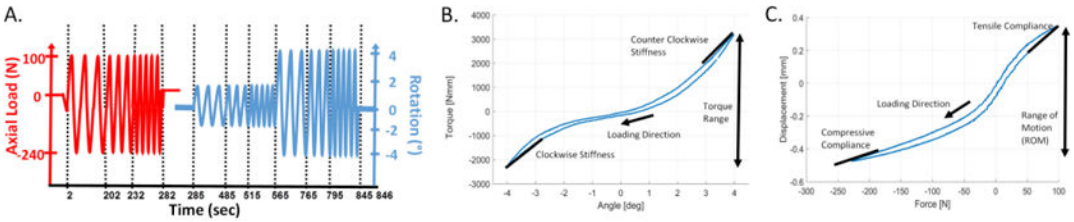


**Figure 1. Repeated measures study design for assessing biomechanical response of intact, injured and repaired ovine intervertebral discs (IVDs)**

(A) IVDs from five cervical levels (C2:C7) from nine animals were distributed to two groups in a repeated measures study design. (B) The cervical IVDs were distributed to two groups independent of level. (C) IVDs distributed to Injured and FibGen groups were tested in the Intact condition and injured with 2- mm biopsy punch. IVDs in the Injured group were tested after injury. IVDs in FibGen group were repaired with injection of FibGen and tested.

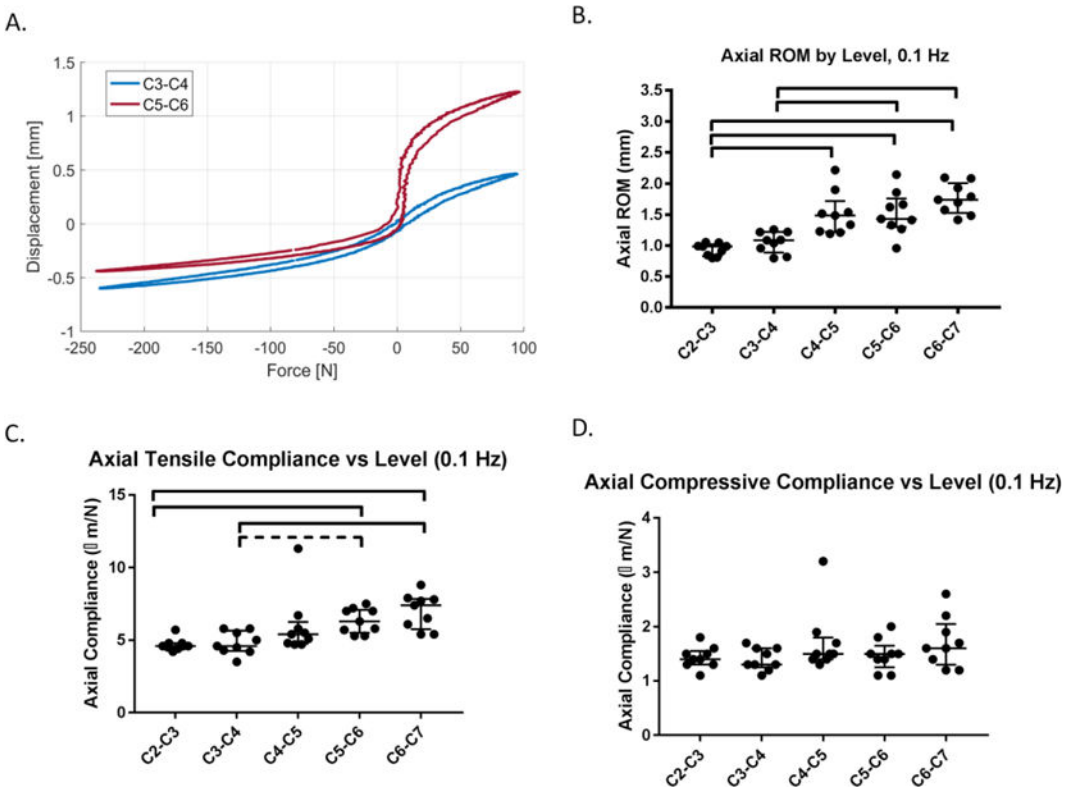


**Figure 2. Biomechanical testing procedures and parameter definitions for torsional and axial biomechanical testing**

(A) The torque range was calculated as the peak to peak torque between ± 2° and ± 4°; the stiffness was slope of top 20% of the torque rotation curve at ± 2° and ± 4° which was averaged for clockwise and counter-clockwise stiffness values. (B) The range of motion was the total displacement between the common applied load for that frequency (for 0.1 Hz, 94 N and -227 N); the axial compliance was the slope of 20% of the displacement force curve.

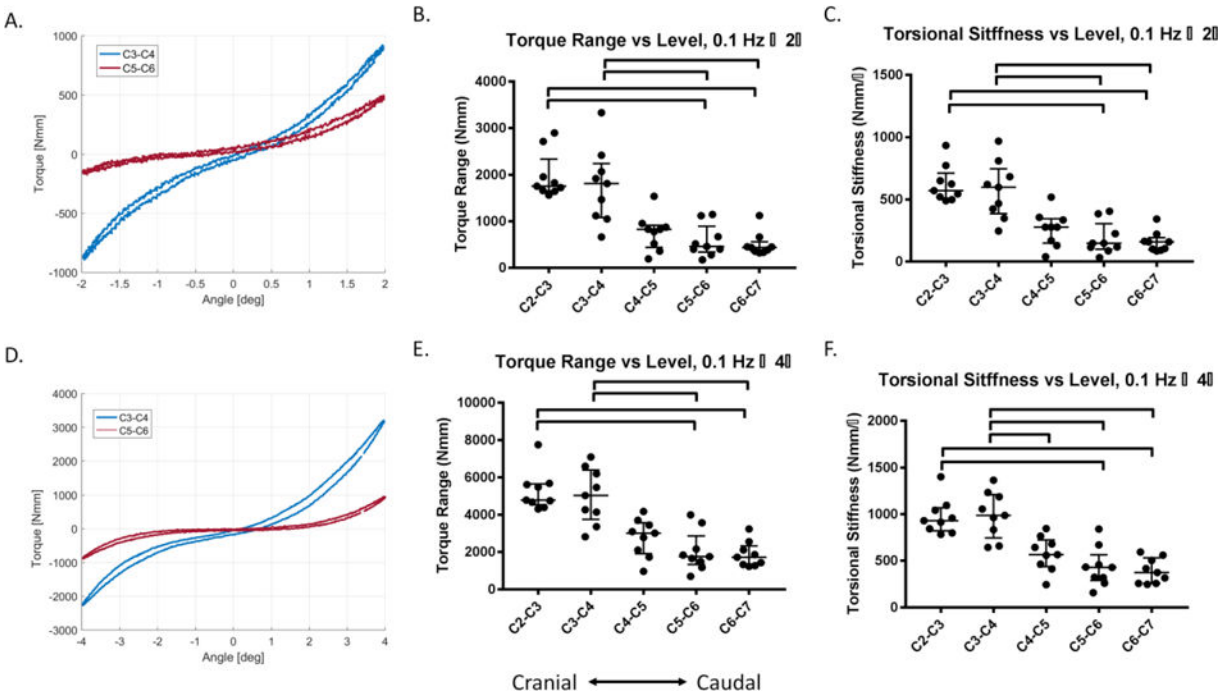


**Figure 3. The two cranial (C2-C3 & C3-C4) motion segments (n = 9/level) have different axial response than the two most caudal levels (C5-C6 & C6-C7)**

(A) The force displacement curve of a C3-C4 motion segment has lower range of motion (ROM) and lower tensile compliance than the C5-C6 motion segment from the same animal. (B) The axial ROM of C2-C3 & C3-C4 were significantly lower than C5-C6 & C6-C7, and the ROM of C2-C3 was significantly lower than C4-C5. (C) The tensile compliance for C2-C3 was significantly lower than C5-C5 and C6-C7, and C3-C4 was significantly lower than C6-C7 but was only a trend lower than C5-C6 ($p = 0.09$). There were no differences in compressive compliance between levels. Lines are median, error bars are interquartile range and bars indicate significant difference ($p < 0.05$).

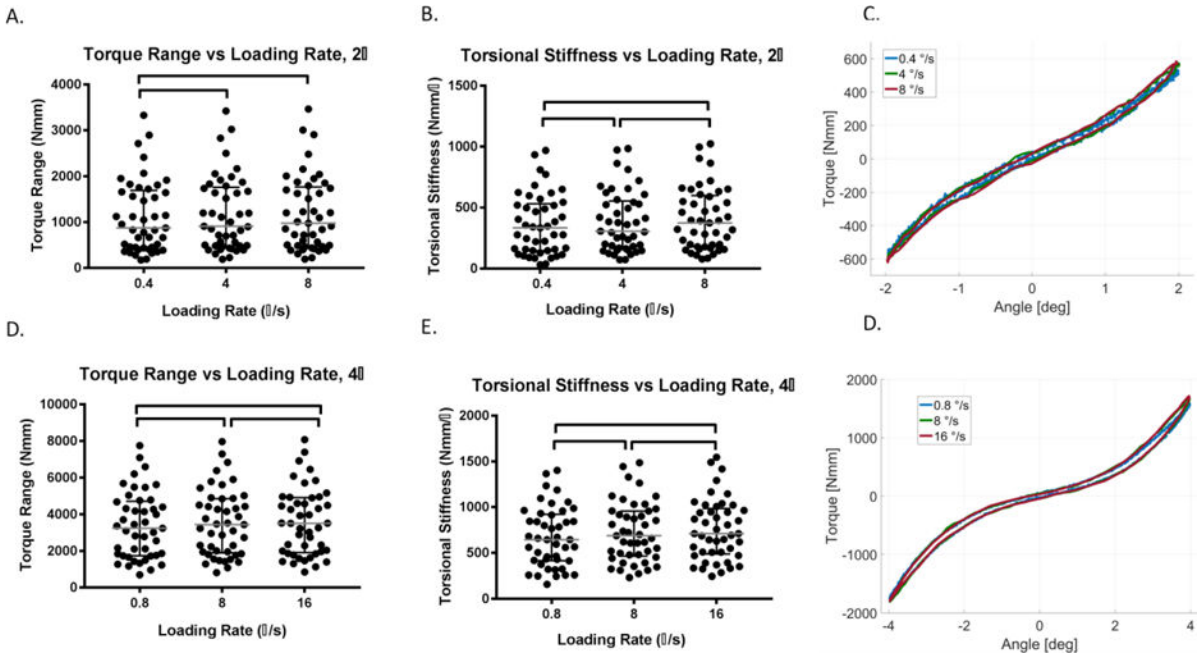


**Figure 4. The two cranial (C2-C3 & C3-C4) IVDs (n = 9/level) have different torsional response than the two most caudal levels (C5-C6 & C6-C7)**

(A) The torque-rotation curve for ± 2° rotation at 0.1 Hz of a C3-C4 motion segment has higher torque range and torsional stiffness than the C5-C6 motion segment from the same animal. (B) The torque range between ± 2° of the two most cranial levels (C2-C3 & C3-C4) were significantly higher than two most caudal levels (C5-C6 & C6-C7) at 0.1 Hz. (C) The torsional stiffness at ± 2° of C2-C3 and C3-C4 was significantly greater than C5-C6 & C6-C7. (D) The torque rotation curve for ± 4° rotation at 0.1 Hz of a C3-C4 motion segment has higher torque and torsional stiffness than the C5-C6 motion segment from the same animal. (E) The torque range between ± 4° of the two most cranial levels (C2-C3 & C3-C4) were significantly higher than two most caudal levels (C5-C6 & C6-C7) at 0.1 Hz. (F) The torsional stiffness at ± 4° of the C2-C3 and C3-C4 levels were significantly greater than C5-C6 and C6-C7, and C3-C4 had significantly greater torsional stiffness than C4-C5. Lines are median, error bars are interquartile range and bars indicate significant difference ($p < 0.05$).

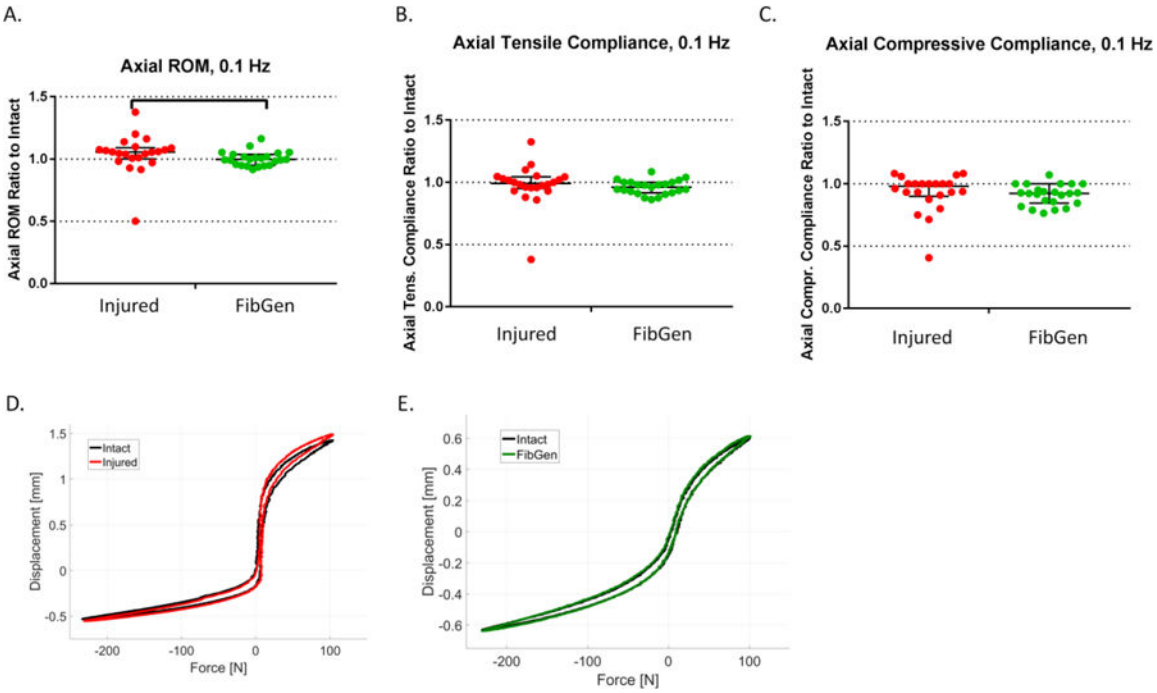


**Figure 5. Torsional loading rate (n = 45) increased torque range and torsional stiffness**

(A) For rotation of ± 2°, the torque range of 0.4 °/s loading was significantly lower than for 4 °/s and 8 °/s. (B) The torsional stiffness at ± 2° was significantly higher for each increasing loading rate from 0.4 °/s to 4 °/s and 8 °/s. (C) Representative torque rotation curves at 0.4, 4 and 8 °/s shows the median change in torque range and torsional stiffness. (D) For rotation of ± 4°, the torque range was significantly higher for each increasing loading rate from 0.8 °/s to 8 °/s and 16 °/s. (E) The torsional stiffness at ± 4° was significantly higher for each increasing loading rate from 0.8 °/s to 8 °/s and 16 °/s. (F) Representative torque rotation curves at 0.8, 8 and 16 °/s shows the median change in torque range and torsional stiffness. Lines are median, error bars are interquartile range and bars indicate significant difference ($p < 0.05$).

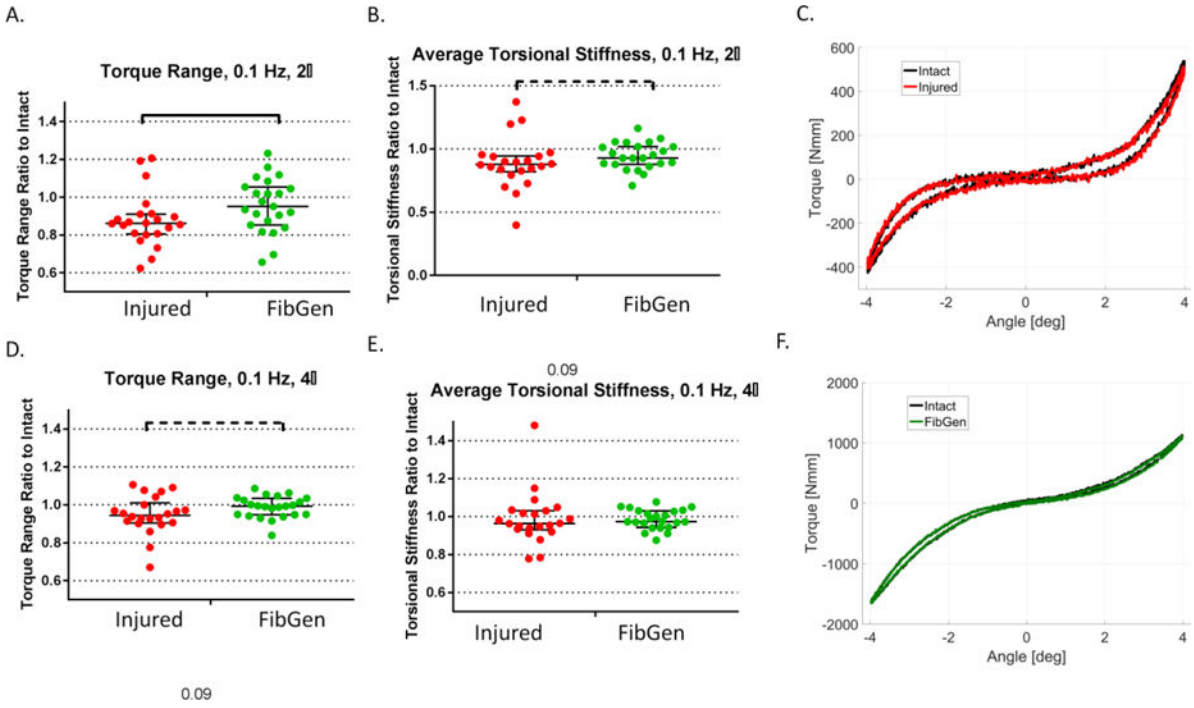


**Figure 6. Annulus injury altered some parameters of axial biomechanical response relative to intact more than the FibGen repair**

(A) The range of motion (ROM) (ratio to intact) of the Injured group was higher than the FibGen group. (B) The tensile compliance ratio and (C) compressive compliance ratio did not differ between groups. (D) Representative force displacement curves of an Injured sample in intact (black) and injured (red) condition shows median effect of injury on axial ROM. (E) Representative force displacement curves of a FibGend sample in intact (black) and repaired (green) condition shows median effect of repair on axial ROM. Lines are median, error bars are interquartile range and bars indicate significant difference ($p < 0.05$).

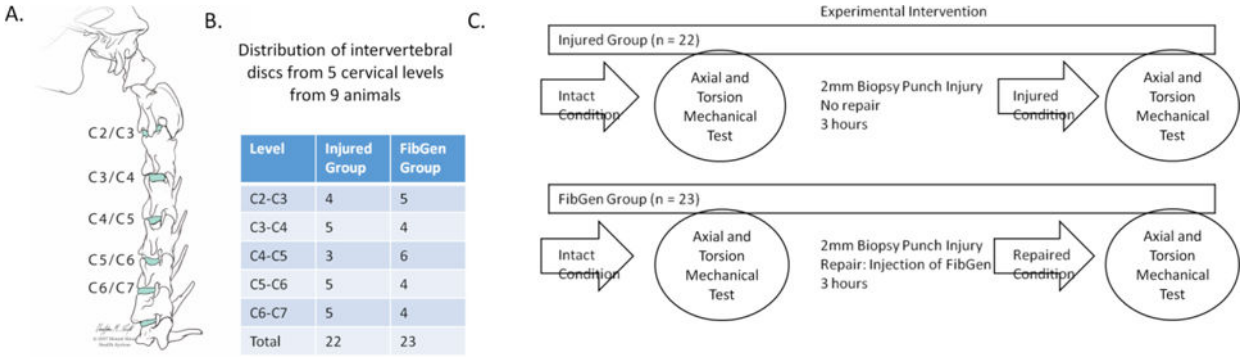


**Figure 7. Annulus injury altered torsional biomechanical properties relative to intact and FibGen repair restored some of these changes**

(A) The ± 2° torque range (ratio to intact) of the Injured group was higher than the FibGen group. (B) The torsional stiffness of the Injured group had a trend of increase compared to the FibGen group ($p < 0.1$). (C) Representative ± 2° torque rotation curves of an Injured sample in intact (black) and injured (red) condition shows median effect of injury on torque range. (D) The ± 4° torque range ratio of the Injured group had a trend of increase compared to the FibGen group ($p < 0.1$). (E) The ± 4° torsional stiffness ratio did not differ between groups. (F) Representative ± 4° torque rotation curves of a FibGen sample in intact (black) and repaired (green) condition shows median effect of injury on torque range. Lines are median, error bars are interquartile range, bars indicate significant difference ($p < 0.05$) and dashed line bars indicate trends ($p < 0.10$).